Document downloaded from:

http://hdl.handle.net/10251/81842

This paper must be cited as:

Solsona Espriu, BE.; López Nieto, JM.; Agouram, S.; Soriano Rodríguez, MD.; Dejoz, A.; Vázquez, MI.; Concepción Heydorn, P. (2016). Optimizing both catalyst preparation and catalytic behaviour for the oxidative dehydrogenation of ethane of Ni-Sn-O catalysts. Topics in Catalysis. 59(17-18):1564-1572. doi:10.1007/s11244-016-0674-z.

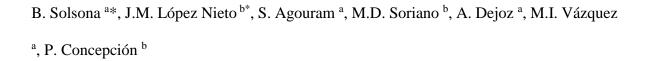


The final publication is available at http://doi.org/10.1007/s11244-016-0674-z

Copyright Springer Verlag (Germany)

Additional Information

Optimizing both catalyst preparation and catalytic behaviour for the oxidative dehydrogenation of ethane of Ni-Sn-O catalysts



- a) Department of Chemical Engineering, ETSE, Universitat de València, 46100
 Burjassot, Spain.
- b) Instituto de Tecnología Química (UPV-CSIC), Campus de la Universidad Politécnica de Valencia, Avenida de los Naranjos s/n, 46022 Valencia, Spain.
- * To whom correspondence should be addressed: jmlopez@itq.upv.es

Benjamin.solsona@uv.es;

Abstract

Bulk Ni-Sn-O catalysts have been synthesized, tested in the oxidative dehydrogenation

of ethane and characterized by several physicochemical techniques. The catalysts have

been prepared by evaporation of the corresponding salts using several additives, i.e.

ammonium hydroxide, nitric acid, glyoxylic acid or oxalic acid, in the synthesis gel. The

catalysts were finally calcined at 500°C in air. Important changes in the catalytic

behaviour have been observed depending on the additive. In fact, an important

improvement in the catalytic performance is observed especially when some additives,

such as glyoxylic or oxalic acid, are used. Thus the productivity to ethylene multiplies by

6 compared to the reference Ni-Sn-O catalyst if appropriate templates are used, and this

is the result of an improvement in both the catalytic activity and the selectivity to ethylene.

This improved performance has been explained in terms of the decrease of the crystallite

size (and the increase in the surface area of catalyst) as well as the modification of the

lattice parameter of nickel oxide.

Keywords: nickel; tin; metal oxides catalysts; oxidative dehydrogenation; ethylene;

oxalic acid; glyoxylic acid.

2

1. INTRODUCTION

In the last ten years, metal-promoted nickel oxides have been intensively studied as catalysts for the oxidative dehydrogenation (ODH) of ethane [1-18] especially those related to Ni-Nb-O metal oxides [2-4, 6-10, 12]. In fact, nickel oxide presents a low selectivity to ethylene (from 10 to 30% at conversion lower than 30%), depending on catalyst preparation procedure [1-18]. Moreover, promoted [1-13] or supported [14-18] nickel oxide changes the catalytic behavior in terms of activity and selectivity. A clear example is observed in the case of Ni-W-O in which the reaction network for ethane ODH strongly changes depending on Ni/W atomic ratio [5]: i) parallel and consecutive reactions takes place (with the formation of ethylene, CO and CO₂, and with overoxidation of ethylene) are observed over Ni-poor catalysts (in which Ni-tungstate is mainly observed); and ii) parallel reaction (with the formation of ethylene and CO₂, and without overoxidation of ethylene) are observed over Ni-rich catalysts (in which NiO is mainly observed).

A similar trend has been also proposed in the case of the promoted- or supported-NiO catalysts [1-18], with NiO as the main crystalline phase, in which low variations in the selectivity to ethylene with the ethane conversion is observed (at least at ethane conversions lower than 30%). Moreover, a strong influence of the addition of various promoters on the nature of active sites has been observed where only few metal oxides have shown a positive promoter effect. Thus, correlations between the valence of the promoter and the selectivity to ethylene [4] or between the acid-base character of the dopant cation and the selectivity to ethylene [10] have been also proposed, niobium [2-4, 6-10, 12] and tin [11, 12] being the most effective promoters of NiO.

In both cases, the crystal size of the NiO particles has been shown to decrease.

Accordingly, crystal size of NiO have been ascribed to have an important influence on

selectivity to ethylene (catalysts presenting small crystals sizes of NiO particles show a better selectivity to ethylene than those presenting bigger crystal sizes [12]). In addition to these, the nature of Ni species have been shown to change also depending on the metal oxide promoter [2, 5, 8, 10], being non-stoichiometric Ni species involved in ethane oxidation to carbon oxides, whereas stoichiometric Ni²⁺ species seems to be involved in the selective oxidative transformation of ethane to ethylene. Additionally, CO [11, 12] and methanol sorption studies [10], electrical conductivity [13] and ¹⁶O₂/¹⁸O₂ isotopic exchange experiments [2, 8, 10-12] suggest that the presence of dopants could modify the amount of electrophilic oxygen species which are generated on surface defects.

In view of these data, the aim of our study is to improve the catalyst performance of Ni-Sn-O catalysts by modifying the catalyst preparation procedure. In this sense, the catalysts have been prepared using different additives. The influence of the preparation method on their physicochemical properties has been analyzed using several characterization techniques, and their catalytic properties tested in the ethane ODH.

2. EXPERIMENTAL

Ni-Sn-O mixed metal oxides catalysts were prepared through the evaporation at 60 °C of a stirred ethanolic solution of nickel nitrate, Ni(NO₃)₂.6H₂O (Sigma–Aldrich), and tin (II) oxalate, SnC₂O₄ (Sigma– Aldrich). A theoretical Ni/Sn atomic ratio of 12 was used in all cases. In a first part, an additive (i.e., ammonium hydroxide, nitric acid, oxalic acid or glyoxylic acid) was also added to the ethanolic solution, with an additive/Ni molar ratio of 1.3.

In a second part, and using oxalic acid as additive, the oxalic acid/Ni molar ratio was also varied (i.e. Oxalic acid/Ni molar ratio of 0, 0.13, 0.39, 0.65, 1.3 or 2.65). The solids were

dried overnight at 120 °C and finally calcined in static air for 2 h at 500 °C. Nomenclature and physicochemical properties of these catalysts are shown in Table 1.

Characterization of the catalysts

Catalyst surface areas were determined by multi-point N_2 adsorption at -196 °C. The data were treated in accordance with the BET method.

Powder X-ray diffraction (XRD) was used to identify the crystalline phases present in the catalysts. An Enraf Nonius FR590 sealed tube diffractometer, with a monochromatic CuKα1 source operating at 40 kV and 30 mA was used.

Temperature-programmed reduction (TPR) was carried out in a Micromeritics Autochem 2910 equipped with a TCD detector, in which the reducing gas was 10% H_2 in Ar (total flow rate of 50 ml min⁻¹). The temperature range explored was from room temperature to 800 °C. The heating rate was maintained at 10 °C min⁻¹.

Morphological, compositional and structural analysis of mixed oxides samples were performed by high resolution transmission electron microscopy (HRTEM) with a field emission gun TECNAI G2 F20 microscope operated at 200 kV, having the capabilities of selected area electron diffraction (SAED) and energy dispersive X-ray spectroscopy (EDX). The elemental composition and distribution of nickel have been determined by using EDX-mapping. In order to prepare the TEM samples, the powdered samples were treated by sonicating in absolute ethanol for several minutes, and a drop of the resulting suspension was deposited onto a holey carbon film supported on a copper grid, which was subsequently dried.

X-ray photoelectron spectroscopy (XPS) measurements were performed on a SPECS spectrometer equipped with a Phoibos 150 MCD-9 detector using monochromatic AlKα (1486.6 eV) X-Ray source. Spectra were recorded using analyzer pass energy of 30 V, an

X-ray power of 100 W and an operating pressure of 10⁻⁹ mbar. Spectra treatment has been performed using the CASA software. Binding energies (BE) were referenced to C1s at 284.5 eV.

Catalytic test for ethane oxydehydrogenation

The catalytic tests in ethane oxidation were carried out in a tubular isothermal flow reactor in the 250–400 °C temperature range. The feed corresponds to a mixture consisting of C₂/O₂/He with a molar ratio of 3/1/29. Typical reaction conditions used were 0.5 g of catalyst and 25 ml min⁻¹, although both the catalyst amounts loaded and the total flows used were largely varied to achieve different ethane conversions at a given reaction temperature. Samples were introduced in the reactor diluted with silicon carbide in order to keep a constant volume in the catalytic bed. Reactant and products were analyzed by gas chromatography using two packed columns: (i) molecular sieve 5A (2.5 m); and (ii) Porapak Q (3 m). Ethylene and carbon dioxide were the main reaction products detected regardless of the catalysts tested. CO was also identified but generally with low selectivity. The catalytic data shown in the present article are the average of the results obtained in two analyses with a stabilization time of 30 min each one. Blank runs showed no conversion in the range of reaction temperatures employed [12].

3. RESULTS AND DISCUSSION

3.1. Catalytic results for ethane oxidative dehydrogenation

The catalytic studies for ethane ODH of these samples led to different catalytic results although in all cases high selectivity to ethylene was observed (Table 2). Figure 1 compares the catalytic performance of the reference catalyst (i.e. **NS** sample) with those achieved over catalysts prepared in the presence of additives. In all cases, an enhanced

performance was observed in terms of both catalytic activity and selectivity to ethylene. Thus, the catalysts prepared with additives showed a reaction rate at least twice that achieved by the reference. It is noteworthy the catalyst treated with glyoxylic acid, led to the highest activity, 6 fold than that of the reference. If considered the specific activity (activity per surface area of the catalyst, in 10^{-3} g_{C2} m⁻² h⁻¹) it can be seen that the reference catalyst shows a similar value than that of the catalyst treated with nitric acid (NS-NA) or those prepared with high oxalic acid/Ni molar ratios. However, catalysts prepared with oxalic acid/Ni molar ratio of 0.13 to 0.65 present a specific activity at least 2 times that of the reference catalyst and those prepared with ammonium hydroxide or glyoxylic acid present a specific activity 3 times that of the reference catalyst.

Regarding the selectivity it must be mentioned that in the conversion range studied (until 25%) the drop of the selectivity to ethylene with the ethane conversions was very low for all the catalysts tested. The lowest selectivity to ethylene was obtained with the reference catalysts (ca. 75%) whereas the highest value corresponded to that prepared with oxalic acid (ca. 85%).

Due to the highest selectivity observed with **NS-OA-4** (and also to the remarkable higher activity compared to the reference catalyst) we decided to undertake a more detailed study about the influence of the amount of oxalic acid used in the preparation method of Ni-Sn-O catalysts and their catalytic performance. Figure 2 shows comparatively the catalytic performance of samples prepared in the presence of oxalic acid. Figure 2a shows the variation of catalytic activity per gram of catalyst or per surface area with the oxalic acid/Ni molar ratio in the synthesis gel. For the optimal catalyst **NS-OA-3** (oxalic acid/Ni molar ratio 0.65) the activity reported is ca. 5 times higher than that of the reference catalyst. However, no important changes are observed at higher oxalic acid/Ni molar ratio. On the other hand, Figure 2b presents the variation of the selectivity to ethylene

with the ethane conversion at isothermal conditions (through modifying the contact time). A flat trend is observed for all the catalysts suggesting the low potential of these catalysts for ethylene decomposition. It can be observed that adding small loadings of oxalic acid, the selectivity to ethylene has been continuously growing until an oxalic/Ni mol ratio of 0.65, reaching selectivity to ethylene as high as 89%. Higher oxalic acid contents leads to slightly lower selectivity (ca. 85%) but still higher than that of the sample without oxalic (ca. 75%). Accordingly, the addition of oxalic acid has facilitated, in all cases, an improvement in the catalytic performance in the oxidation of ethane (Figure 2).

The catalytic stability of two representative catalysts, NS and NS-OA-3, was studied with the time-on-stream for 12 h. A slight decrease of the catalytic activity (ca. 10%) was observed in both cases. It must be noted that most of the deactivation was observed for the first two hours on line.

3.2. Characterization of catalysts

Figure 3 shows the XRD patterns of Ni-Sn-O catalysts. As it can be seen in all cases the same peaks were detected. The most intense peaks correspond to (111), (200) and (220) family plane of NiO (JCPDS: 78-0643) and other less intense of SnO₂ (JCPDS: 41-1445) were also detected. Both the intensity and the width of the peaks vary depending on the catalyst. Thus, the reference Ni-Sn-O catalyst and that prepared with ammonium hydroxide presented the lowest widths and consequently the largest crystallites.

Figure 3b shows the XRD patterns of samples prepared with the presence of oxalic acid in the synthesis gel. It can be seen widening of the NiO peaks with the presence of oxalic acid which means a decrease in both the crystallite size (Fig. 4a) and the lattice parameter "a" (Fig. 4b) in NiO. However for oxalic acid/Ni mol/atom ratios higher than 1.3 further increments in the concentration of oxalic acid did not further decrease the crystallite size

(nor lattice parameter "a"). Accordingly, a similar trend in both the particle size and the lattice parameter of NiO crystallites with the oxalic acid content in the synthesis gel can be proposed.

In addition to changes in the crystal size of NiO, changes in the surface area of catalysts depending on the additive used have been also observed. Thus the presence of an additive as ammonium hydroxide hardly affect both the surface area (ca. 42 m² g¹) and the NiO crystallite size (ca. 23 nm) compared to the reference **NS** catalyst (Table 1). However, the addition of nitric acid increases 2-fold of the surface area with the subsequent decrease in the NiO crystallite size (ca. 8 nm). In a similar way, the use of oxalic and glyoxylic acids led to an enhanced surface area (97 and 83 m²/g, respectively) and crystallite sizes of ca. 8 and ca. 11 nm, respectively. It must be indicated that in the case of samples prepared in the presence of oxalic acid, the surface area of the catalysts strongly depends on the oxalic acid/Ni ratios showing a maximum value of 96.6 m²g¹¹ at an oxalic acid/Ni ratio of 1.3. Further increases in the oxalic acid loading decrease slightly the surface area (see Table 1). Probably an excess of oxalic acid does not participate in the mechanism for a further decrease of the NiO crystallite size.

Figure 5 shows the temperature programmed reduction profiles for these catalysts. In the reference catalyst, i.e. NS sample, a broad band centered at ca. 378°C related to the reduction of NiO (and Ni³⁺) was observed [19, 20]. If the synthesis is carried out in the presence of nitric acid or oxalic acid similar profiles were observed but slightly shifted towards lower temperatures (ca. 370 and 360°C, respectively). The shift of the peak must be likely related to the lower NiO crystallite size of the treated catalysts. Differences in the interactions between NiO particles and tin oxide particles can also be accounted for the shift observed [11].

Different profiles are observed in the case of the samples prepared in the presence of ammonium hydroxide (with two bands apparent at 320/375°C) or glyoxylic acid (with two bands apparent at 320/375°C). These bands can be related to the reduction of Ni²⁺ or Ni³⁺ to metallic nickel in different environments [19, 20].

In the case of catalysts prepared in the presence of oxalic acid, the TPR profiles show a band with two shoulders which relative intensity depends on the catalyst. The first shoulder is less intense and appears at ca. 300°C whereas the second one is most intense and centered at ca. 345-358°C. Thus, the presence of oxalic acid in the synthesis gel leads to an enhanced reducibility of the corresponding Ni-species.

Table 1 shows the H₂ consumptions in the TPR experiments undertaken until 800°C. Similar H₂-uptake was observed in all cases suggesting non important changes in the oxidation state of Ni-species [11].

The results of XPS analyses of SnO₂-promoted NiO catalysts are summarized in Table 3, while Figure 6 shows the evolution of the Ni2p3/2 core level spectra of the NS-OA-series. Clear differences in the Ni2p3/2 XPS peak symmetry were observed according to the oxalic acid amount in the synthesis gel. In general, the Ni2p3/2 XPS peak shows three components, at ca. 854.3, 856.4 and 861.4 eV, which can be referred as the main peak (854.3 eV) and the satellite peaks (856.4 and 861.4 eV) [5,11]. The satellite peak at 861.4 eV has been associated to the charge transfer ligand—metal [21], whereas the satellite peak at ca. 856.4 eV has been related as a consequence of a non-local screening mechanism [21] due to the presence of Ni²⁺ vacancies [22], or to Ni²⁺-OH species [23] or Ni³⁺ ions [24].

The intensity ratio of both satellites peaks versus the main-peak gives very useful information about the nature of sites [5,11]. Accordingly, differences in the local environment of the Ni atoms can be inferred, in which the different unsaturation degree

depends on the use or not of additives in the synthesis gel and on the amount of oxalic acid used.

For a better understanding of these catalysts a detailed microscopy study was undertaken. Figure 7 presents transmission electron images of Ni-Sn samples with different oxalic acid loadings. As we can observe in high magnification TEM, it is clear that the samples present two types of nanoparticles with two different grain size, one present small nanoparticles with size in the order of 2 nm and others with size ranging from 5 to 20 nm. Both of them consist of homogeneous and nearly spherical grains. An aggregation of smaller particles is also observed. TEM micrographs show a decrease in the grain size of Ni particles when increasing the oxalic acid loading of the catalyst. Thus in the case of the oxalic acid free NS sample particles in the 10-50 nm range are mainly observed whereas for NS-OA-4 sample most particles are in the 5-20 nm range. Figure 8 shows a detailed study for the NS-OA-3 sample. EDX-maps indicate the coexistence of both metals (Sn and Ni) in the analyzed area. Also we can observe that the Ni-containing crystal is well dispersed while Sn-containing crystals present some agglomerations. This same trend was observed for all the samples analyzed. SAED patterns show that the samples consist of crystalline nanoparticles of Ni that could be indexed to the NiO and a few to SnO₂. As previously reported, some shift in the XRD measured lattice parameter was observed when increasing the oxalic acid loading until NS-OA-3 while higher oxalic acid loadings did not further affect the lattice parameter value (see Figure 4b). These decreases in the lattice parameter could be attributed to low grain size of nanoparticles and or to the incorporation of a small quantity of Sn in the NiO matrix. In fact, as the control of the beam position and spot size is possible in our TEM microscope operating in nanoprobe mode, the chemical composition in selected NiO nanoparticles of the samples was achieved and results in the existence of a small quantity of Sn-atoms in the

measured nanoparticles. All samples were analyzed by EDX in nanoprobe mode revealing that the composition of smaller nanoparticles is rich in tin (about 50 % at. of Ni and 50 % at. of Sn) while the biggest ones are rich in nickel (98-99% at. of Ni and 1-2 % of Sn). This agrees with quantitative XPS results (see table 3), where a higher Ni/Sn ratio is observed on the NS-OA-1 sample showing the biggest crystal size, while a decrease in the Ni/Sn ratio is detected at decreasing NiO crystal size.

Comparing catalytic results with characterization data, the catalysts prepared with additives showed a reaction rate higher than that observed over the reference catalyst (i.e. **NS** sample). This enhanced activity could be partially related to the higher surface area of the catalysts with additives. In addition, if the specific activity (per surface area) is considered the values are also higher. Accordingly, this enhanced specific activity can be also related to the higher reducibility of catalysts prepared in the presence of additives. Thus, the catalyst with the highest activity presents the reduction profile at the lowest temperatures. However the trend for the other catalysts is not so clear.

In the case of the selectivity to ethylene we have observed a trend between the variation of the selectivity to ethylene with both the lattice parameter (Fig. 9a) and the crystallite size (Fig.9b) of NiO particles; in a way that lowers lattice parameters and NiO crystallite size, the higher is the selectivity (Fig. 9c). We must indicate that the presence of relatively low surface acidity has a strong influence on the catalytic performance of Sn-promoted NiO catalysts [11], since the presence of acid sites can be related to the decomposition of the ethylene formed. Accordingly, the results presented suggest that both lattice parameter and the crystallite size of NiO particles could have a strong influence on the selectivity to ethylene as proposed previously for other promoted NiO catalysts [11, 12]. It is clear that, in these cases, a higher interaction between NiO and SnO₂ particles could

also be favored. The decrease in both the catalytic activity and selectivity to ethylene observed when the oxalic acid loading is high is not easy to explain. However we think it is related to the lower amount of nickel on the surface as detected by XPS. Nickel sites are the main active sites in the ethane activation and a decrease of the surface Ni concentration can lead to a lower catalytic activity. At low oxalic acid contents the amount of surface nickel decreases when the amount of oxalic acid increases but, at the same time, a decrease in the crystallite size takes place. However after oxal/Ni ratios of 0.65-1.3 the crystallite size does not decrease any more, and then the lower amount of surface nickel sites involves a lower activity. Moreover, at high oxalic acid loadings the amount of exposed tin sites increases and this can be related to the lower selectivity to ethylene as it is known [11] that Sn oxide is hardly selective to ethylene.

4. Conclusions

Ni-Sn-O catalyst with a Ni/Sn atomic ratio of 12 is active and selective in the oxidative dehydrogenation (ODH) of ethane. However, both activity and selectivity can be modified by incorporating additives in the synthesis gel. In this case, oxalic acid seems to have an interesting effect on both activity and selectivity, but this effect change with the oxalic acid/Ni ratio in the synthesis gel. This improved performance can be explained in terms of both an increase in the surface area of catalyst and a decrease of the crystallite size (as well as the modification of the lattice) parameter of nickel oxide.

The optimized catalysts show higher surface area and higher reducibility and lower alattice parameter and crystal size of NiO. In addition the optimized catalysts present also changes in the nature of Ni species on the catalyst surface as proposed from the XPS results. As a consequence for the optimized catalyst with oxalic acid presents an ethylene production rate ca. 6 times higher than the catalyst without oxalic acid and this is the consequence of both a higher catalytic activity and a higher selectivity to ethylene.

Acknowledgments

The authors would like to acknowledge the DGICYT in Spain (CTQ2012-37925-C03-1, and CTQ2012-37925-C03-2) for financial support. We also thank the University of Valencia and SCSIE-UV for assistance.

References

- 1. Heracleous E, Lee AF, Wilson K, Lemonidou AA (2005) J Catal 231:159-171.
- 2. Heracleous E, Lemonidou AA (2006) J Catal 237:162-174.
- 3. Savova B, Loridant S, Filkova D, Millet JMM (2010) Appl Catal A Gen 390:148-157.
- 4. Heracleous E, Lemonidou AA (2010) J Catal 270:67-75.
- Solsona B, Lopez Nieto JM, Concepcion P, Dejoz A, Ivars F, Vazquez MI (2011) J Catal 280:28-39.
- 6. Skoufa Z, Heracleous E, Lemonidou AA (2012) Catal Today 192:169-176.
- Zhu H, Ould-Chikh S, Anjum DH, Sun M, Biausque G, Basset JM, Caps V
 (2012) J Catal 285:292-303.
- 8. Skoufa Z, Heracleous E, Lemonidou AA (2012) Chem Eng Sci 84:48-56.
- Zhu H, Rosenfeld DC, Anjum DH, Caps V, Basset JM (2015) ChemSusChem 8:1254-1263.
- 10. Heracleous E, Lemonidou AA (2015) J Catal 322:118-129.
- 11. Solsona B, Concepcion P, Demicol B, Hernandez S, Delgado JJ, Calvino JJ, Lopez Nieto JM (2012) J Catal 295:104-114.

- 12. Lopez Nieto JM, Solsona B, Grasselli RK, Concepción P (2014) Top Catal 57:1248-1255.
- Popescu I, Skoufa Z, Heracleous E, Lemonidou AA, Marcu IC (2015) PCCP 17:8138-8147.
- 14. Zhang X, Gong Y, Yu G, Xie Y (2002) J Mol Catal A Chem 180:293-298.
- 15. Popescu I, Skoufa Z, Heracleous E, Lemonidou A, Marcu I-C (2015) Phys Chem Chem Phys 17:8138-8147.
- 16. Nakamura KI, Miyake T, Konishi T, Suzuki T (2006) J Mol Catal A Chem 260: 144-151.
- 17. Solsona B, Dejoz AM, Vazquez MI, Ivars F, Lopez Nieto JM (2009) Top Catal 52:751-757.
- 18. Bortolozzi JP, Gutierrez LB, Ulla MA (2013) Appl Catal A Gen 452:179-188.
- 19. Takeguchi T, Furukawa S, Inoue M (2001) J. Catal 202:14-24.
- 20. Richardson JT, Turk B, Twigg M.V (1996) Appl Catal. A Gen 148:97-112.
- 21. Biju V, Abdu Khadar M (2002) J Nanopart Res 4:247-253.
- 22. Van Veenendaal MA, Sawatzky GA (1993) Phys Rev Lett 70:2459-2462.
- 23. Vedrine JC, Hollinger G, Duc TM (1978) J Phys Chem. 82:1515-1520.
- 24. Salagre P, Fierro JLG, Medina F, Sueiras JE (1996) J Mol Catal A 106: 125-134.

Table 1. Physico-chemical characteristics of Ni-Sn-O catalysts (Ni/Sn ratio= 12), prepared in the presence or absence of additives.

Catalyst ^a	Additive	Additive/Ni	$S_{ m BET}$	TPR re	esults
		Mol. ratio	(m^2g^{-1})	H ₂ uptake ^b	TMC ^c
NS	-	-	42.3	17.14	378
NS-NH	Ammonia	1.3	42.2	17.32	375
NS-NA	Nitric acid	1.3	87.8	17.25	359
NS-GA	Glyoxylic acid	1.3	83.3	16.80	295
NS-OA-1	Oxalic acid	0.13	57.1	17.11	358
NS-OA-2	Oxalic acid	0.39	72.3	16.90	348
NS-OA-3	Oxalic acid	0.65	87.9	16.70	350
NS-OA-4	Oxalic acid	1.3	96.6	17.24	357
NS-OA-5	Oxalic acid	2.65	82.3	16.92	355

a) Calcined at 500°C; b) in mmol/g; c)

Table 2. Catalytic performance in the oxidative dehydrogenation of ethane of Ni-Sn-O catalysts (Ni/Sn ratio= 12), prepared in the presence or absence of additives. ^a

Catalyst	W/F b	Ethane Conversion	Selectivity to	Selectivity to	STY c	Catalytic	Specific
		(%)	ethylene (%)	CO ₂ (%)		Activity d	activity e
NS	82	12.3	75.6	24.4	31.8	42.1	1.07
NS-NH	33	11.8	77.4	22.6	78.0	108	2.56
NS-NA	33	11.8	82.1	15.9	82.8	108	1.23
NS-GA	12.5	12.2	79.6	20.4	218	294	3.53
NS-OA-1	41	15.8	81.2	18.8	87.7	116	2.03
NS-OA-2	21	10.2	84.1	15.9	117	149	2.07
NS-OA-3	16	12.2	88.5	11.5	185	223	2.50
NS-OA-4	41	11.9	84.3	15.7	68.6	87.2	0.90
NS-OA-5	41	14.3	85.0	15.0	83.1	105	1.27

a) Reaction conditions in text: reaction temperature = 350 °C; b) Contact time, W/F, in g_{cat} h $(mol_{C2})^{-1}$; c) **STY**, space—time yield in g_{C2H4} k g_{cat}^{-1} h⁻¹; d) Catalytic Activity for ethane conversion in g_{C2H6} k g_{cat}^{-1} h⁻¹; e) in 10^{-3} g $_{C2}$ m⁻² h⁻¹

Table 3. XPS analysis of Ni-Sn-O catalysts.

Sample	Ni/Sn	Ni2p3/2	Sn3d5/2				
	surface ratio	Main peak	Satellite S(I)	Satellite S(II)	S(I)/MP a	S(II)/MP a	Main peak
		(eV)	(eV)	(eV)			(eV)
NS	10.0	853.9	855.8	861.1	1.46	1.22	486.6
NS-OA-1	18.7	853.7	855.7	860.9	1.51	1.72	486.6
NS-OA-3	6.7	854.0	856.0	861.2	1.45	1.52	486.6
NS-OA-5	4.6	854.3	856.1	861.1	1.52	1.63	486.6

 $[\]textbf{a)} \quad \text{Satellite/main-peak intensity ratio, considering } S(I) \text{ or } S(II) \text{ as satellite peak.}$

Caption to figures

Fig. 1. Catalytic activity for ethane conversion and selectivity to ethylene for Ni-Sn-O catalyst prepared in the presence of additives in the synthesis gel. Notes: Reaction conditions detailed in text. T = 350°C. Selectivity at a conversion of ethane of 10%. Catalytic activity per g of catalyst (in g_{C2} Kg_{cat}^{-1} h^{-1}) as in Table 1.

Fig. 2. Catalytic performance in ethane oxidation of Ni-Sn-O catalysts prepared in the presence of oxalic acid as additive in the synthesis gel. a) Variation of the Catalytic Activity, in g_{C2} kg_{cat}^{-1} h^{-1} (open symbols), and Specific Activity, in 10^{-3} g_{C2} m^{-2} h^{-1} (filled symbols), with the oxalic acid used in the preparation procedure; b) Variation of the selectivity to ethylene with ethane conversion at a reaction temperature of 350 °C. Notes: Reaction conditions detailed in text; reaction temperature.

Fig.3. XRD patterns of Ni-Sn-O catalysts: a) Samples prepared in the absence (NS) and in the presence of ammonium hydroxide (NS-NH); nitric acid (NS-NA); glyoxylic acid (NS-GA); or oxalic acid (NS-OA-4); b) Samples prepared in the presence of oxalic acid with different Oxalic acid/Ni molar ratio (see table 1).

Fig. 4. Variation of the crystal size of NiO particles (a) and variation of the lattice parameter "a" of NiO crystals (b) with the Oxalic acid/Ni molar ratio in the synthesis gel.

Fig. 5. Temperature-programmed reduction patterns of: a) Samples prepared in the absence (NS) and in the presence of ammonium hydroxide (NS-NH); nitric acid (NS-NA); glyoxylic acid (NS-GA); or oxalic acid (NS-OA-4); b) Samples prepared in the presence of oxalic acid with different Oxalic acid/Ni molar ratio (see table 1).

Fig. 6. X-ray photoelectron spectra of Ni2p3/2 of Ni-Sn-O catalysts prepared with a oxalic acid/Ni ratio in the synthesis gel of: 0 (NS), 0.13 (NS-OA-1); 0.65 (NS-OA-3); 2.45 (NS-OA-5).

Fig. 7. TEM images for Ni-Sn-O catalysts prepared with oxalic acid/Ni molar ratio in the synthesis gel of: a) 0 (NS), b) 0.13 (NS-OA-1), c) 0.65 (NS-OA-3), d) 2.45 (NS-OA-4).

Fig. 8. Low magnification TEM micrographs, its corresponding selected area electron diffraction (SAED) pattern and Ni (in green) and Sn (red) EDX-mapping of NS-OA-3 catalyst.

Fig. 9. Variation of the selectivity with the crystallite size (a) and the a-lattice parameter (b) of NiO and variation of a-lattice parameter of NiO with the corresponding crystallite size. Notes: Reaction conditions detailed in text. $T = 350^{\circ}$ C. Selectivity at a conversion of ethane of 10%.